

## **An application of dynamic deformation model in to the Barium isotopes**

<sup>1</sup>Saad N. Abood and <sup>2</sup>Ghofran A. Ali

*Physics Department, College of Science, AL-Nahrain University, Baghdad, Iraq*

---

### **ABSTRACT**

*In this work, the ground state, quasi gamma and quasi beta band energies of <sup>120140</sup>Ba isotopes have been investigated by using the Dynamic Deformation Model (DDM). In calculations, the theoretical energy levels have been obtained by using DDM program codes. The presented results are compared with the experimental data in respective tables and figures. At the end, it was seen that the obtained theoretical results are in good agreement with the experimental data.*

**Key words:** Dynamic Deformation Model, Even-Even Ba, Band Energies (Ground State, Quasi Gamma and Quasi Beta Band).

---

### **INTRODUCTION**

Interest in the  $A = 130$  region of light Ba isotopes ( $N < 82$ ) was renewed in 1985 on the recognition that some of these nuclei are good examples of the  $O(6)$  dynamic symmetry of the Interacting Boson Model (IBM) [1]. Later, in 2000, with the identification of <sup>134</sup>Ba as a good example of the newly proposed analytically solvable  $E(5)$  critical point symmetry on the  $U(5)-O(6)$  path by Iachello [2], and by Casten and Zamfir [3], interest in the Ba isotopes ( $N < 82$ ) was renewed. Kumar and Gupta [4] extended the highly successful microscopic theory in the dynamic pairing plus quadrupole (DPPQ) model of Kumar-Baranger [5] to the  $A = 130$  region, by using the appropriate Nilsson spherical single-particle energies, and applied it to the study of the neutron-deficient Ba isotopes.

Puddu *et al.*, [6] used the Interacting Boson Model (IBM-2) to predict the general trend of variation with  $N$  of the level structures and E2 moments in Xe, Ba and Ce ( $N < 82$ ). Castanos *et al.*, [7] derived the effective Hamiltonian in IBM-1 in terms of Casimir operators with seven adjustable coefficients to study the groups of nuclei including light Ba isotopes. In Ba they obtained  $2_\gamma$  below  $4_g$  for all  $N$ , contrary to experiment. Hamilton *et al.*, [8] studied the  $\gamma$  decay from the  $2_3^+$  state at about 2-MeV excitation in the nuclei <sup>140</sup>Ba, <sup>142</sup>Ce, and <sup>144</sup>Nd, with 84 neutrons and is shown to be consistent with its identification as the lowest state of mixed symmetry in the  $U(5)$  limit of the neutron-proton version of the interacting-boson model.

Novoselsky and Talmi [9] used a larger boson energy  $\varepsilon$  on shell model considerations in IBM-2 application. They kept  $\chi$  the coefficient of  $[dd^\dagger]$  term constant and varied coefficients of other terms in the IBM Hamiltonian to better reproduce the odd-even spin staggering. Sevrin *et al.*, [10] added the  $SU(3)$  term to  $O(6)$  to generate some rigid triaxiality in IBM-2 to better reproduce the odd-even spin staggering in the  $K = 2^+\gamma$ -band. Kumar and Gupta (2001) [11] employed the dynamic pairing plus quadrupole model of Kumar and Baranger for studying variations of the nuclear structure of light Ba isotopes with  $A = 122-134$ . The potential energy surface parameters have been calculated and the low-spin level spectrum is predicted along with the static and transition E2 moments. Comparison with experiment and with other theories supports the validity of our treatment.

Gupta in 2013 [12] The shape-phase transition at  $N = 88-90$ , and the role of  $Z = 64$  subshell effect therein has been a subject of study on empirical basis and in the context of the  $Np - Nn$  scheme, but a microscopic view of the same has been lacking. The dynamic pairing plus quadrupole model (DPPQ) is employed to predict the occupation

probabilities of the neutron and proton deformed, single-particle orbitals. The nuclear structure of Ba–Dy ( $N > 82$ ) nuclei is studied and the shape equilibrium parameters derived.

The objective of the present study is to test the capabilities of DDM model and to give an insight on the variation of the nuclear structure and electromagnetic transitions of  $^{120-140}\text{Ba}$  with neutron number  $N$ . We have done a detailed study of the energy systematics of  $^{120-140}\text{Ba}$  and the  $E2$ ,  $M1$  transition rates in their decay, mixing ratios  $\delta(E2/M1)$ .

Our work represents an attempt in the dynamic deformation model for analyzing the nuclear structure of Ba isotopes varying with neutron number  $N$ . We give a brief account of our method and we present the results and compare a large amount of data with experiment. We discuss the successes and the limitations of our method and give our conclusions.

**2- Dynamic Deformation Model (DDM)**

The dynamic deformation model has been developed over many years starting from the Paring Plus Quadrupole model (PPQ) of Kumar and Baranger [13]. The DDM is an ambitious attempt to the collective spherical-transitional-deformed transitions and to span from the s-d shell to heavy nuclei using a microscopic theory of collective motion. No fitting parameters are required to obtain the data for a particular nucleus.

A full description of the DDM is given in reference [14] and references therein. Here we present only the results of our application of the new version [33] of the DDM to the tellurium isotopes.

The detailed formalism and early results may be found in Kumar *et al.*, [14] and Kumar [15]. Here we give briefly the main aspects of the model. The theory can be divided into two main parts: a microscopic derivation of a collective Hamiltonian, and a numerical solution of the Hamiltonian. The microscopic Hamiltonian is composed of a demoralized Nilsson-type single particle plus pairing and has the form:

$$H = H_{av} + V_{res} \dots\dots\dots(1)$$

Where

$$H_{av} = \frac{p^2}{2M} + \frac{1}{2}M \sum_{k=1}^3 \omega_k^2 \chi_k^2 + \hbar\omega_0 [v_{ls} l \cdot s + v_{ll} (l^2 - \langle l^2 \rangle_N)] \dots\dots\dots(2)$$

Combining all the various contributions together, the potential energy is written as:

$$V_{coll} = V_{DM} + \delta U + \delta V_{proj} + \delta E_{pair} \dots\dots\dots(3)$$

where  $\delta V_{proj}$  is a nine-dimensional projection correction introduced by Kumar [15]. The generalized cranking method is employed to derive the general expression for mass parameters  $B_{\mu\nu}(\beta, \gamma)$  as used in the collective kinetic energy which can be written as:

$$T_{coll} = \frac{1}{2} \sum_{\mu\nu} B_{\mu\nu} \alpha_\mu \alpha_\nu^* \dots\dots\dots(4)$$

This kinetic energy function is quantized by Pauli method.

The DDM code used for our calculation is a modified version of the latest DDM code which was developed for super-heavy nuclei. The single particle levels and the configuration space ( $n = 0$  to 8) employed in the present calculation, as well as the deformation definition, are identical to those of Kumar *et al.*, [14]. The main virtues of the above approach (restoration of symmetries, unified treatment of spherical-transitional-deformed nuclei) have recently been combined with the main virtues of the Nilsson-Strutinsky approach (large configuration space, no effective charges, applicability to fission isomers and barriers) in the Dynamic Deformation Model (DDM).

The GCM (general coordinate motion) wave function is written as [15]:

$$\Psi_{\alpha,l}(q) = \int \Phi_\alpha(q, \beta) f_{\alpha,l}(\beta) d \dots\dots\dots(5)$$

where  $I$  is total nuclear angular momentum,  $a$  distinguishes states with the same  $I$ ,  $q$  represents all the nucleonic variables, and  $\beta$  represents all the collective variables. The expectation value of the nuclear Hamiltonian  $H$  is then given by

$$\langle \alpha I | H | \alpha I \rangle = \iint d\beta' f_{\alpha I}(\beta') h(\beta, \beta') f_{\alpha, I}(\beta) d\beta \dots \dots \dots (6)$$

where  $h(\beta, \beta')$  is the expectation value of  $H$  with respect to the nucleonic variables. The "double" integral of Eq. (6) is replaced in the DDM by a "single" integral. The function  $h(\beta, \beta')$  is expanded in the non-locality with respect to deformation,

$$h(\beta', \beta) = h_0(\beta) \delta(\beta' - \beta) + h_1(\beta) \delta'(\beta' - \beta) + h_2(\beta) \delta''(\beta' - \beta) + \dots \dots \dots (7)$$

The formal derivation has been given by Giraud and Grammaticos [16]. Although a complete derivation of the formalism used in the PPQ model or the DDM (or the cranking method combined with the Bohr Hamiltonian method) is not claimed, the conceptual connection is quite clear and precise, and is briefly the following: The  $h_0$  term of Eq. (7) leads to the potential energy  $V$  of the collective Hamiltonian. The  $h_1$  term vanishes because of the symmetry requirements. The  $h_2$  term leads to the kinetic energy,  $T = (1/2) \dot{\beta}^* \cdot B \cdot \dot{\beta}$  of the collective Hamiltonian, where  $B$  is the mass-parameter-matrix. This matrix is given by:

$$B_{\mu, \nu} = \partial^2 T / (\partial \dot{\beta}_\mu^* \partial \dot{\beta}_\nu^*) = \partial^2 H / (\partial \dot{\beta}_\mu^* \partial \dot{\beta}_\nu^*) \dots \dots \dots (8)$$

The collective velocities  $\dot{\beta}_\mu^*$  may represent  $\beta$ -vibrations,  $\gamma$ -vibrations, pair fluctuations, or rotational frequencies. The original cranking method of Inglis dealt with only one of these, the frequency of rotation around an axis perpendicular to the assumed symmetry axis or the nuclear spheroid. Then, the connection between the time-dependent Schrodinger equations in the laboratory system and in the intrinsic system gives the  $\omega$ -dependence of the Hamiltonian,  $H' = H - \omega J_x$ . We generalize this to obtain [17]:

$$H' = H - \frac{\hbar}{i} \sum_\mu \dot{\beta}_\mu^* \frac{\partial}{\partial \beta_\mu} \dots \dots \dots (9)$$

Then, the second-order time-dependent perturbation theory gives the 'cranking' type of formulae for the mass-parameter-matrix  $B_{\mu\nu}$ . Note that the following constraint conditions are satisfied automatically up to second order in  $\dot{\beta}_\mu^*$  [15]:

$$\frac{\hbar}{i} \left\langle \frac{\partial}{\partial \beta_\mu} \right\rangle = \sum_\nu B_{\mu\nu} \dot{\beta}_\nu^* \dots \dots \dots (10)$$

These conditions include the traditional 'cranking' constraint,  $\langle J_x \rangle = \Theta \omega$ , as a special case.

In the current version of the DDM, the adiabatic approximation is made that the collective velocities/frequencies are small compared to those of the single-particle motion, that is [15]

$$\hbar \omega_{rot} \ll \hbar \omega_{sp} = 41 A^{-1/3} MeV \dots \dots \dots (11)$$

$$\hbar \omega_{vib} \ll \hbar \omega_{sp} = 41 A^{-1/3} MeV \dots \dots \dots (12)$$

However, this adiabatic approximation is far superior to that of the rotational model where some additional approximations are made ( $\omega_{rot} \ll \omega_{vib}$ , harmonic vibrations with amplitudes much smaller than the equilibrium deformation value). The rotation-vibration coupling is treated exactly in the DDM by avoiding any expansions around the equilibrium shapes, by calculating the potential and inertial functions microscopically for each point of a  $\beta - \gamma$  mesh, and by solving the collective Schrodinger equation by numerical method [18,19,20].

## RESULTS AND DISCUSSION

## 3-1 Energy Spectra

The even-mass Barium isotopes ( $Z=56$ ) are part of an interesting region beyond the closed proton shell at  $Z=50$  where the level structure has resisted detailed theoretical understanding. The present investigation of the Barium isotopes,  $N=64-84$ , mainly by the dynamic deformation model is a part of a wider study which includes tellurium, xenon and selenium.

The calculated collective energy levels of the tellurium isotopes were obtained by changing the value of  $N$  over the range  $N=64-80$  without adjusting any parameters in the model. The Dynamic Deformation Model (DDM) calculated level energies are presented in Figs. (1) to (10). The basic features of the variation of level structure with neutron number  $N$  are well reproduced. In the ground state band the variation of the energy ratio  $E(4_1^+)/E(2_1^+)$  from a value of 2.927 in  $^{120}\text{Ba}$  at neutron number  $N=64$  to 2.098 in  $^{136}\text{Ba}$  at neutron number  $N=80$  is reproduced.

The variation of  $E(2_1^+)$  and  $E(4_1^+)$  increased gradually with increasing neutron number, i.e., the variation of the moment of inertia with  $N$  is reproduced. The crossing of the state  $2_2^+$  below  $4_1^+$  in  $^{132-134}\text{Ba}$  isotopes at  $N=76-78$  is obtained, as one goes from  $N=46$  to  $N=80$ . Similarly the  $0_2^+$  state is below  $4_1^+$  in  $^{136}\text{Ba}$  at  $N=76$  and the  $0_2^+$  state is below  $3_1^+$  state in  $^{124-136}\text{Ba}$  isotopes and lies at high energy in  $^{130-136}\text{Ba}$  isotopes.

The gamma band ( $2_2^+, 0_2^+, 4_2^+$ ) lies high  $^{122-136}\text{Ba}$  isotopes. Also the states  $2_3^+$  and  $3_1^+$  lies high. The levels  $2_3^+$ ,  $2_4^+$ ,  $0_3^+$ ,  $4_3^+$ ,  $4_4^+$  comparison with experimental has to be done carefully.

Table 1: Experimental and DDM values of energy ratios in Ba isotopes

Isotopes	$E(4_1^+)/E(2_1^+)$		$E(6_1^+)/E(2_1^+)$		$E(2_2^+)/E(2_1^+)$		$E(0_2^+)/E(4_1^+)$		$E(0_2^+)/E(2_1^+)$	
	Exp.	DDM								
$^{120}\text{Ba}$	2.924	2.927	5.592	5.218	-	6.807	-	2.485	-	6.612
$^{122}\text{Ba}$	2.902	2.747	5.543	5.166	3.155	6.797	-	2.294	-	6.303
$^{124}\text{Ba}$	2.834	2.640	5.342	4.833	3.798	5.690	1.378	1.885	3.921	4.978
$^{126}\text{Ba}$	2.777	2.516	5.204	4.462	3.412	4.132	1.382	1.660	3.839	4.177
$^{128}\text{Ba}$	2.687	2.389	4.953	4.113	3.114	2.806	1.234	1.552	3.316	3.780
$^{130}\text{Ba}$	2.523	2.287	4.456	3.844	2.540	2.806	1.307	1.517	3.302	3.470
$^{132}\text{Ba}$	2.427	2.181	4.159	3.551	2.220	2.118	1.333	1.306	3.239	2.849
$^{134}\text{Ba}$	2.316	2.185	3.656	3.512	1.931	2.225	1.257	1.229	2.911	2.675
$^{136}\text{Ba}$	2.280	2.098	2.696	3.260	1.894	2.108	0.845	1.830	1.929	3.841
$^{140}\text{Ba}$	1.876	2.001	2.692	3.022	2.507	2.081	1.613	2.485	3.027	3.311

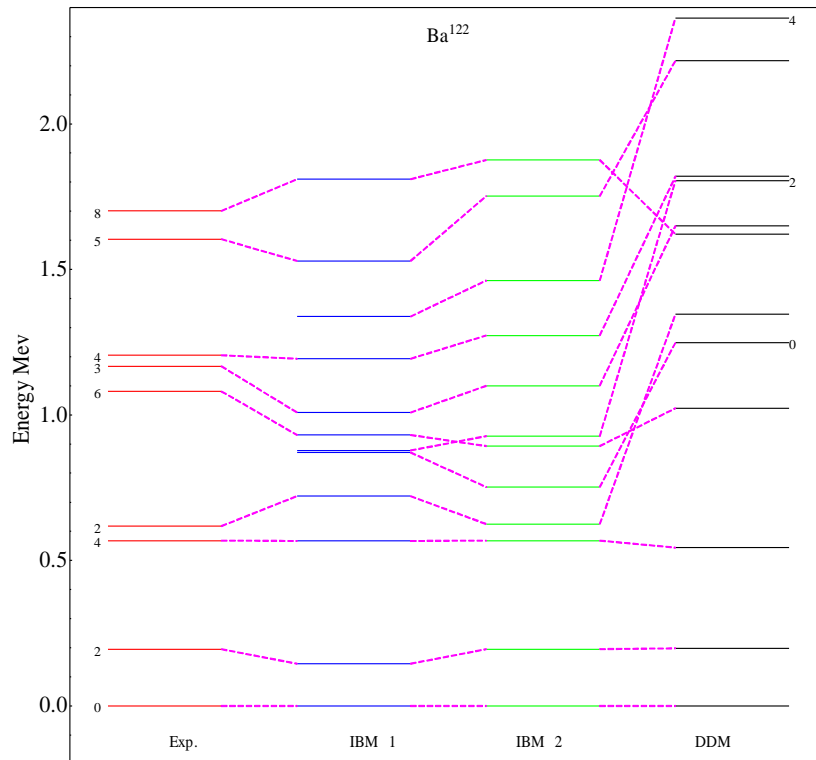


Fig. 1: Comparison between experimental data and DDM calculated energy levels for  $^{120}Ba$

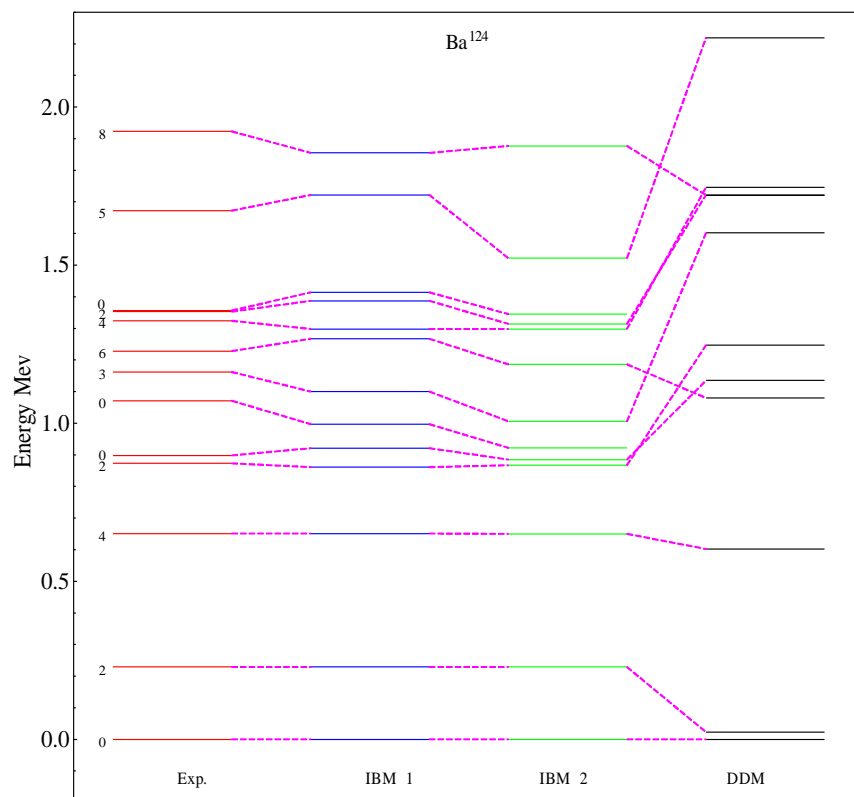


Fig 2: Comparison between Experimental data and DDM calculated energy levels for  $^{122}Ba$

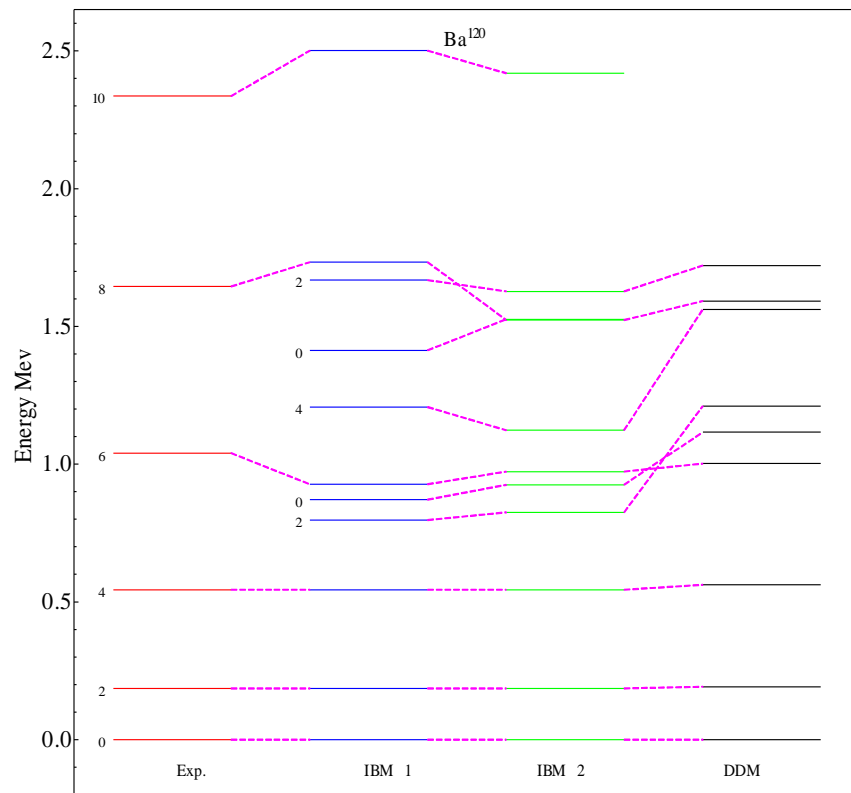


Fig 3: Comparison between experimental data and DDM calculated energy levels for  $^{124}Ba$

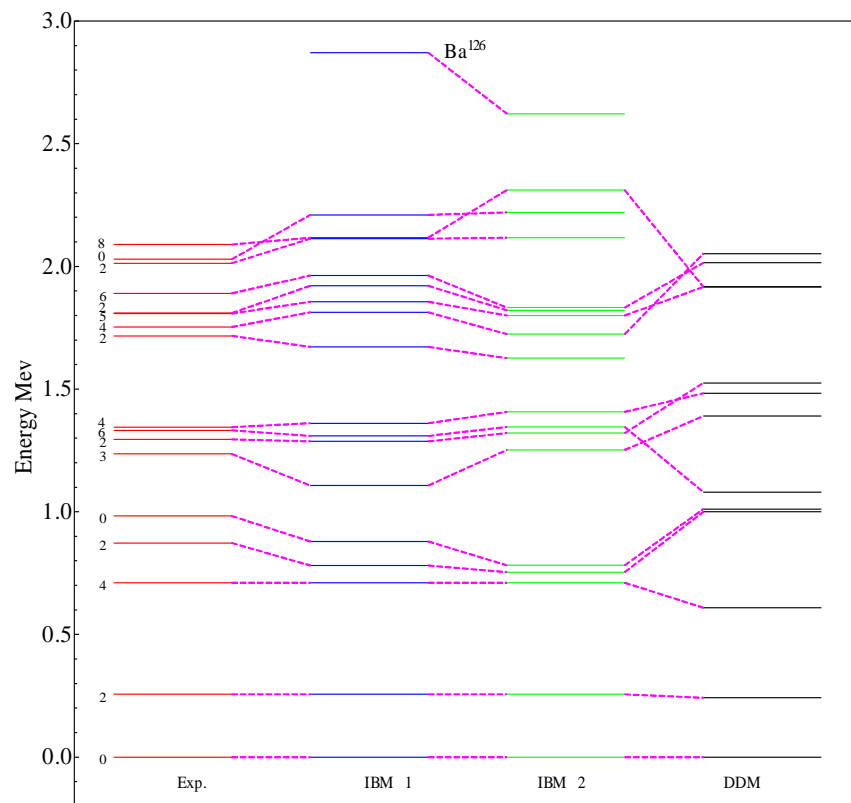


Fig 4: Comparison between experimental data and DDM calculated energy levels for  $^{126}Ba$

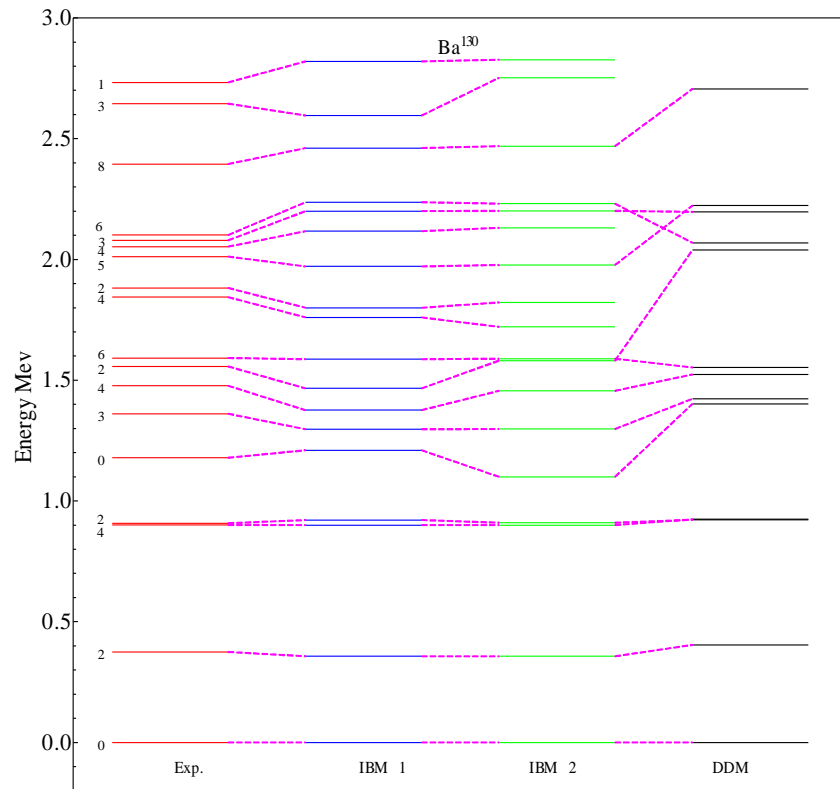


Fig 5: Comparison between experimental data and DDM calculated energy levels for  $^{128}Ba$

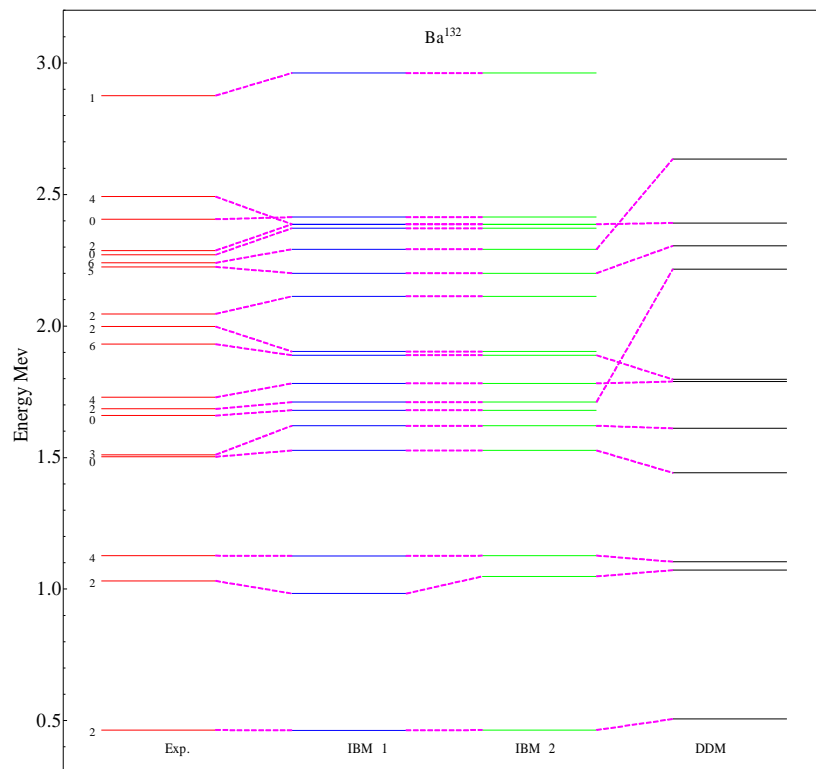


Fig 6: Comparison between experimental data and DDM calculated energy levels for  $^{130}Ba$

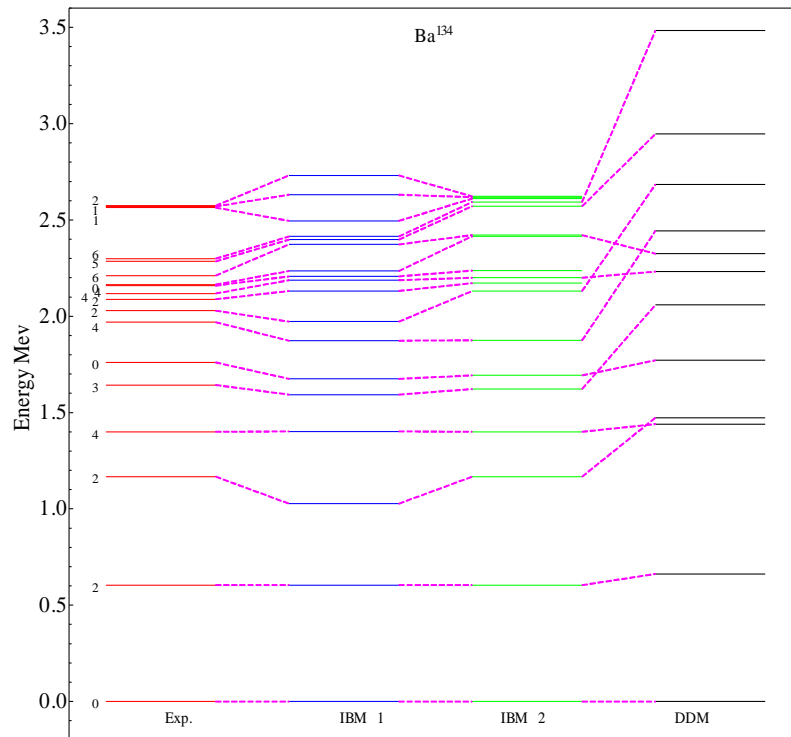


Fig 7: Comparison between experimental data and DDM calculated energy levels for  $^{132}Ba$

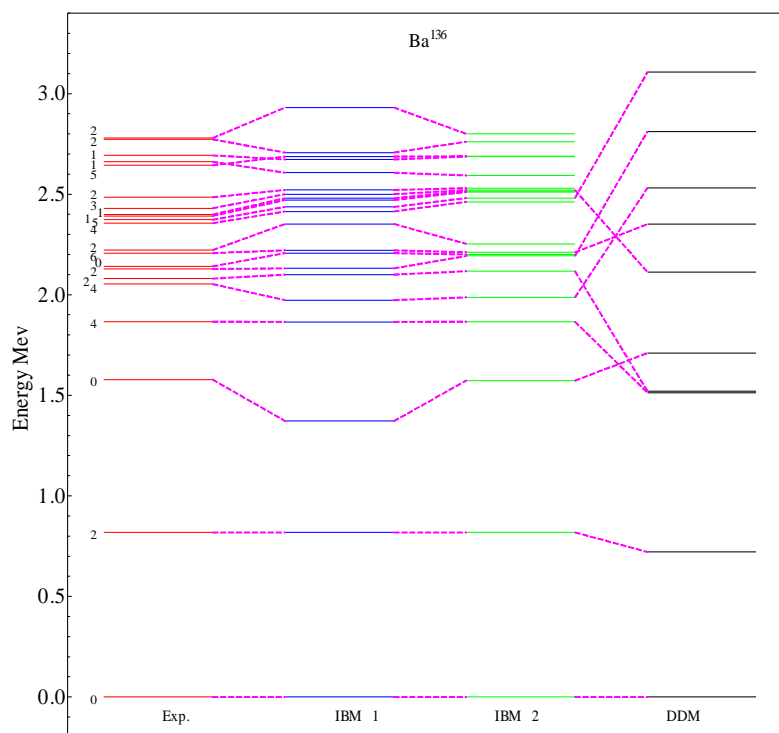


Fig 8: Comparison between experimental data and DDM calculated energy levels for  $^{134}Ba$

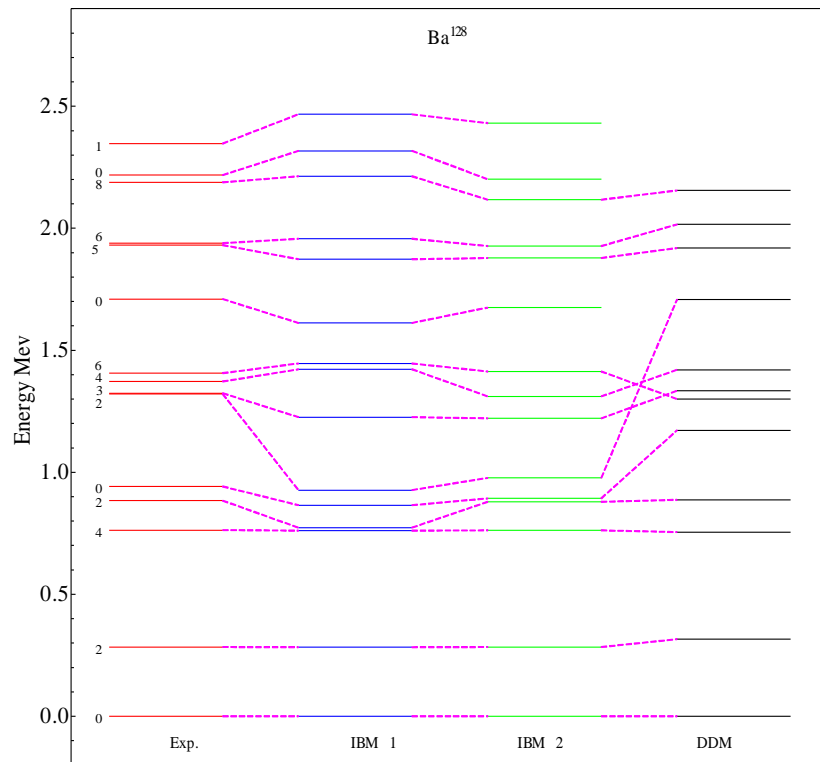


Fig 9: Comparison between experimental data and DDM calculated energy levels for  $^{136}Ba$

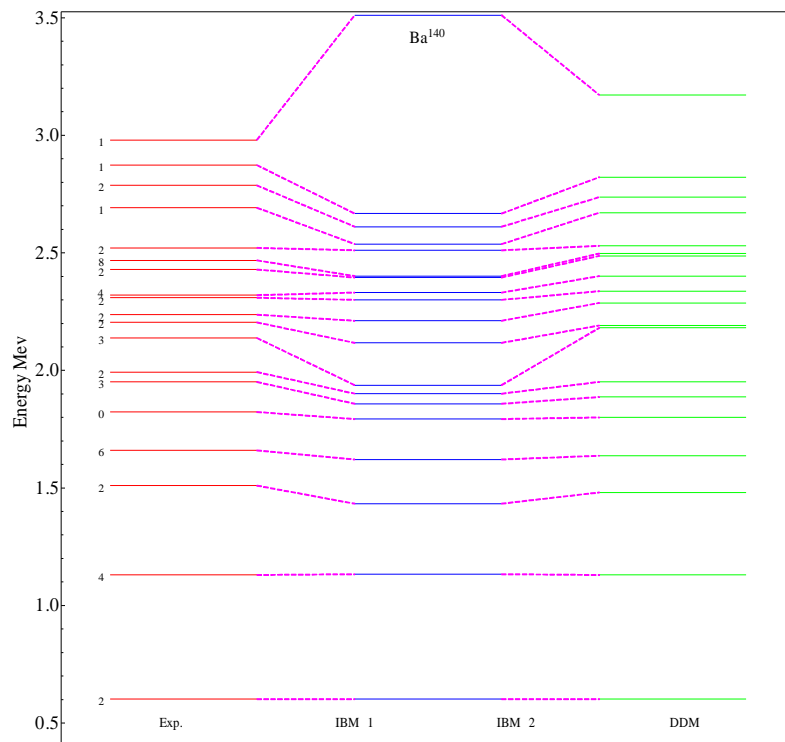


Fig 10: Comparison between experimental data and DDM calculated energy levels for  $^{140}Ba$

Figs. (1) to (10) show the energy levels of the barium isotopes from which we may draw the following conclusions.

(i) The  $E(4_1^+)/E(2_1^+)$  ratio of the level energies decrease from the maximum of 2.927 for  $N=64$  to 2.098 for  $N=80$  (see Table (1)). This indicates a non-collective quasi-particle excitation becoming increasingly important as the neutron number approaches  $N=82$ .

(ii) Both the experimental and calculated  $E(0_2^+)/E(4_1^+)$  ratios indicate that the  $0_2^+$  and  $4_1^+$  levels should occur close together throughout the range of isotopes from  $N=46-80$ . The large values of the ratios  $E(0_2^+)/E(2_1^+)$ , imply stiffness in the collective potential in the  $\beta$  degree of freedom which is consistent with the values in for the deformation energy  $E_d$  (see Table (2)).

In Table (3) DDM calculation for the root-mean-square (rms) values of the deformations parameters  $\beta$  and  $\gamma$  for the ground state  $0_1^+$ , and first excited state  $2_1^+$  and second excited state  $2_2^+$ . These are a nice measure of the shape of the calculated potential energy surface (PES) and its variation with increasing spin or vibrational phonon number [11].

Table 2: Experimental and DDM values of  $\beta_{min}$ ,  $E_d$ ,  $V_{PO}$  energy difference  $E(2_2^+) - E(4_1^+)$  and  $Q(2_1^+)$  in Ba isotopes

Isotopes	$\beta_{min}$		$E_d$		$V_{PO}$		$E(2_2^+) - E(4_1^+)$		$Q(2_1^+)$	
	Exp.	DDM	Exp.	DDM	Exp.	DDM	Exp.	DDM	Exp.	DDM
<sup>120</sup> Ba	-	0.264	-	3.421	-	2.640	-	0.649	-	-1.8
<sup>122</sup> Ba	-	0.266	-	3.320	-	2.470	-	0.802	-1.52(7)	-1.49
<sup>124</sup> Ba	-	0.234	-	2.949	-	2.066	0.222	0.645	-1.31(4)	-1.33
<sup>126</sup> Ba	-	0.237	-	2.411	-	1.477	0.162	0.391	-1.20(4)	-1.26
<sup>128</sup> Ba	-	0.234	-	1.801	-	1.120	0.121	0.132	-1.10(4)	-1.20
<sup>130</sup> Ba	0.23	0.231	-	1.002	-	0.455	0.007	-0.002	-1.02(15)	-1.11
<sup>132</sup> Ba	0.19	0.230	-	0.281	-	0.068	-0.096	-0.032	-0.84(3)	-0.99
<sup>134</sup> Ba	-	-0.082	-	0.062	-	-0.070	-0.233	0.033	-0.31(24)	-0.22
<sup>136</sup> Ba	-	-0.088	-	0.088	-	-0.087	0.027	0.007	-0.19(6)	-0.20
<sup>140</sup> Ba		-0.092	-	0.0097	-	-0.009	0.380	-	-	-0.16

Experimental data are taken from refs. [ 22, 23 ]

Table 3 : The root-mean-square (rms) values of  $\beta$  and  $\gamma$  deformation parameters of ground state and excited states in <sup>120-140</sup>Ba isotopes

Isotopes	$\beta$ Root mean square $\beta_{rms}$			$\gamma$ Root mean square $\gamma_{rms}$		
	$0_1^+$	$2_1^+$	$2_2^+$	$0_1^+$	$2_1^+$	$2_2^+$
<sup>120</sup> Ba	0.265	0.270	26.3 <sup>0</sup>	20.8 <sup>0</sup>	16.4 <sup>0</sup>	26.3 <sup>0</sup>
<sup>122</sup> Ba	0.258	0.266	25.6 <sup>0</sup>	16.8 <sup>0</sup>	15.7 <sup>0</sup>	25.6 <sup>0</sup>
<sup>124</sup> Ba	0.243	0.254	27.3 <sup>0</sup>	18.8 <sup>0</sup>	17.2 <sup>0</sup>	27.3 <sup>0</sup>
<sup>126</sup> Ba	0.224	0.238	29.2 <sup>0</sup>	20.1 <sup>0</sup>	18.8 <sup>0</sup>	29.2 <sup>0</sup>
<sup>128</sup> Ba	0.208	0.223	30.8 <sup>0</sup>	24.9 <sup>0</sup>	22.5 <sup>0</sup>	30.8 <sup>0</sup>
<sup>130</sup> Ba	0.188	0.205	31.3 <sup>0</sup>	27.8 <sup>0</sup>	26.2 <sup>0</sup>	31.3 <sup>0</sup>
<sup>132</sup> Ba	0.157	0.176	30.9 <sup>0</sup>	29.2 <sup>0</sup>	27.7 <sup>0</sup>	30.9 <sup>0</sup>
<sup>134</sup> Ba	0.128	0.152	30.0 <sup>0</sup>	29.4 <sup>0</sup>	30.4 <sup>0</sup>	30.0 <sup>0</sup>
<sup>136</sup> Ba	0.124	0.111	30.3 <sup>0</sup>	28.6 <sup>0</sup>	29.6 <sup>0</sup>	30.3 <sup>0</sup>
<sup>140</sup> Ba	0.098	0.089	31.9 <sup>0</sup>	29.9 <sup>0</sup>	30.6 <sup>0</sup>	31.9 <sup>0</sup>

The root mean square of  $\beta$  ( $\beta_{rms}$ ) value falls with increase in neutron number smoothly or gradually. In a few cases  $\beta_{rms}$  is about 15% lower than  $\beta_{min}$ . This is on account of the sharper rise of potential on the right-hand side (increasing  $\beta$ ) than on the  $\beta = 0$  side [11].

From the Table (3), the values of  $\gamma_{rms}$  for the ground band vary from  $16.4^0$  to  $30.6^0$  and the root mean square of the for  $2_2^+$  state as a member of  $\gamma$ -band lie between  $25.6^0$  and  $31.9^0$ . The values of  $\gamma_{rms}$  show little variation with increasing mass number  $A$ , signifying that the values of PES in DDM here is more symmetrical about the  $\gamma = 30^\circ$ .

### 3-2 Potential Energy Surface

We shall begin our discussion with the  $N = 82$  nucleus and continue to the lighter isotopes. The potential-energy function  $V(\beta, \gamma)$  gives circular contours,  $V(\beta, \gamma) \approx \beta^2$  which are exactly what we expect from the model for a nucleus close to a doubly closed shell. The potential shape of this nucleus is that of a harmonic oscillator with a minimum in the potential at  $\beta = 0$ . In the case of the  $N = 80$  isotope a shallow minimum of  $V(\beta, \gamma) = 0.360$  MeV appears at  $\beta = 0.05$  and  $\gamma = 0$ , but unexpectedly a deep minimum of  $V(\beta, \gamma) = 7.92$  MeV occurs on the oblate axis at  $\beta = 0.092$ . This deep minimum is surprising since only two neutrons have been removed and we might not expect such a dramatic change in the potential from that of the  $N = 82$  nucleus.

In Table (2) the characteristic of potential energy surface (PES), the minimum quadrupole deformation  $\beta_{min}$ , corresponding to the position of the deepest potential minimum are compared with the experimental data and IBM-1 results, the values of  $\beta_{min}$  decrease with increasing neutron number (toward the magic number  $N = 82$ ). In general, we obtain for the values of  $\beta_{min}$  from the Table (2) the deeper prolate minima and shallower secondary oblate minima in all cases, both decreasing in depth with increasing  $N$ . The negative values of  $\beta_{min}$  for  $^{134-140}\text{Ba}$  at  $N = 78, 80$  and  $84$ . At  $^{120}\text{Ba}$  isotope  $N = 64$ , the prolate minimum is 3.250 MeV deep and the oblate minimum is 0.711 MeV deep and lies at lesser  $\beta$  value ( $< \beta_{min}$ ). The same feature continues with increasing neutron number  $N$ . At  $^{134}\text{Ba}$   $N = 78$  we get a very shallow prolate minimum and at  $^{136-140}\text{Ba}$   $N = 80$  and  $84$  a very shallow oblate minimum.

The values of  $V_{PO}$  (Table (2)) the difference in the depth of prolate and oblate minima, is decreasing with increasing neutron number  $N$  in DDM calculation. From these values we obtain the prolate shape for the light Ba isotopes as in IBM-1. At  $^{134-140}\text{Ba}$  isotopes  $N = 78, 80$  and  $84$  the values of  $V_{PO}$  is negative but we obtain almost vanishing prolate and oblate minima [11]. The predicted shape is not a permanently deformed one. In fact the predicted potential well at  $N = 76, 78, 80$  and  $84$  corresponds to the spherical shape (vibrational shape) anharmonic oscillator with flat bottom.

Several trends with increasing mass number ( $A$ ) can be seen in this isotopic chain:

- (i) The magnitude of the deformation and the binding energy of deformation corresponding to the lowest potential minimum decrease.
- (ii) The magnitude of the prolate-oblate difference  $V_{PO}$  decrease in the first half of this region.
- (iii) The deformation at the minimum (the static intrinsic quadrupole moment) changes sign from positive (prolate) to negative (oblate) around  $A = 130$ .

The energy deformation  $E_d$  ( $E_d = V(0) - V_{PO}$ ), decreased with increasing neutron number  $N$  (toward the magic neutron number  $N = 82$ ).

The quadrupole moment of the first excited states  $Q(2_1^+)$  decrease gradually with increasing neutron number. The negative sign signifies prolate shape in  $^{120-140}\text{Ba}$ .

### 3-3 Electric Transition Probability B(E2) and Branching Ratios

The reduced electric transition probabilities for  $^{120-140}\text{Ba}$  isotopes are given in Table (4). Similarly, the reduced transition probabilities  $B(E2; 2_1^+ \rightarrow 0_1^+)$ ,  $B(E2; 4_1^+ \rightarrow 2_1^+)$  and  $B(E2; 6_1^+ \rightarrow 4_1^+)$  decreases with increasing

neutron number  $N$ . The DDM model values vary similarly with experimental data. We see that these criteria provide  $B(E2)$  values for other transitions which agree well with the DDM values and with experimental data except some values for  $B(E2; 2_2^+ \rightarrow 0_1^+)$  transitions in lower neutron number isotopes where the theoretical values in DDM are about a factor of ten too small. These values decrease with increasing  $N$  as expected for decreasing deformation parameter  $\beta$  and increasing the parameter  $\gamma$ .

The transitions  $B(E2; 3_1^+ \rightarrow 2_1^+)$  seem to get weaker with increasing neutron number  $N$ , because the cross over transition (selection rules) indicating the weakening band relationship. The transitions  $B(E2; 2_3^+ \rightarrow 2_1^+)$  and  $B(E2; 0_2^+ \rightarrow 2_1^+)$  in general the values fall with increasing neutron number  $N$ . The experimental value and DDM values in  $^{120-122}\text{Ba}$  isotopes at  $N = 64, 66$  is off the linear rise and needs a recheck, since there is no sudden change of structure in  $^{132-134-136}\text{Ba}$   $N = 66, 68, 70$ . DDM yield a linear rise of  $B(E2)$  with increasing boson number, and reproduces the saturation at mid shell. [24].

A maximum deformation (and associated properties such as deformation energy  $E_d$ ,  $V_{PO}$  and quadrupole moment for first excited state  $Q(2_1^+)$ ) at mid shell is achieved, since the up-sloping orbitals are emptied, while the down-sloping and horizontal orbitals remain filled up with the valence nucleons [11]. Here one must distinguish between the region of nuclei along the  $\beta$ -stability valley and the one across (far from) it as for Ba isotopes ( $A = 130$  nuclei).

The discrepancy of experimental values and theoretical values can be attributed to:

- (i) The round-off errors which are particularly large for those values whose computation involves cancellation of many terms such as forbidden or weak transition rates.
- (ii) Deviations of the calculations from assumed  $Z$  and  $N$  dependence.
- (iii) Deviations from the adiabatic approximation.

**Table 4: Experimental and theoretical values of Electric Transition Probabilities  $B(E2; J_i^+ \rightarrow J_f^+)$  in  $e^2b^2$  Units for Ba isotopes**

Isotopes	$B(E2; 2_1^+ \rightarrow 0_1^+)$		$B(E2; 4_1^+ \rightarrow 2_1^+)$		$B(E2; 6_1^+ \rightarrow 4_1^+)$		$B(E2; 2_2^+ \rightarrow 0_1^+)$		$B(E2; 2_3^+ \rightarrow 0_1^+)$	
	Exp.	DDM	Exp.	DDM	Exp.	DDM	Exp.	DDM	Exp.	DDM
$^{120}\text{Ba}$	-	0.524	-	-	-	0.822	-	0.021	-	0.0043
$^{122}\text{Ba}$	0.54	0.427	-	0.622	-	0.734	-	0.013	-	0.0032
$^{124}\text{Ba}$	0.401	0.381	0.626	0.571	0.64(2)	0.710	-	0.014	-	0.0030
$^{126}\text{Ba}$	0.380	0.311	0.44	0.500	0.49(2)	0.66	-	0.0135	-	0.0028
$^{128}\text{Ba}$	0.276	0.298	0.41(2)	0.432	0.39(3)	0.521	0.13(2)	0.0085	-	0.00282
$^{130}\text{Ba}$	0.230	0.228	0.219	0.329	0.37(2)	0.467	0.15(2)	0.0028	-	0.00261
$^{132}\text{Ba}$	0.158	0.101	0.210	0.301	-	0.368	-	0.0011	-	0.00202
$^{134}\text{Ba}$	0.134(2)	0.077	0.161(18)	0.22	-	0.301	0.0017(5)	0.00082	0.0018(6)	0.0020
$^{136}\text{Ba}$	0.094	0.0542	0.080	0.181	-	0.279	-	0.00065	-	0.00087
$^{140}\text{Ba}$	0.037(34)	-	0.203(18)	-	0.081(4)	-	-	-	-	0.00056

Continued to Table 4

Isotopes	$B(E2;2_3^+ \rightarrow 2_1^+)$		$B(E2;4_1^+ \rightarrow 2_1^+)$		$B(E2;0_2^+ \rightarrow 2_1^+)$		$B(E2;3_1^+ \rightarrow 2_1^+)$	
	Exp.	DDM	Exp.	DDM	Exp.	DDM	Exp.	DDM
$^{120}\text{Ba}$	-	0.023	-	0.076	-	0.076	-	0.093
$^{122}\text{Ba}$	-	0.015	-	0.062	-	0.062	-	0.088
$^{124}\text{Ba}$	-	0.011	-	0.113	-	0.113	-	0.116
$^{126}\text{Ba}$	-	0.00081	-	0.123	-	0.123	-	0.146
$^{128}\text{Ba}$	-	0.0013	-	0.163	-	0.163	-	0.229
$^{130}\text{Ba}$	-	0.0012	-	0.071	-	0.071	-	0.311
$^{132}\text{Ba}$	-	0.00058	-	0.100	-	0.100	-	0.248
$^{134}\text{Ba}$	0.0045(20)	0.00021	-	0.0098	-	0.0098	0.0009(34)	0.193
$^{136}\text{Ba}$	-	0.00020	-	0.0082	-	0.0082	-	0.176
$^{140}\text{Ba}$	-	0.00017	-	0.0081	-	0.0081	-	0.177

Experimental data are taken from Refs. [22, 25, 26, 27, 28, 29, 30]

Branching ratios are given in Table (5). from this table we see the value  $B(E2,2_2^+ \rightarrow 0_1^+)/B(E2;2_2^+ \rightarrow 2_1^+)$ ,  $B(E2,3_1^+ \rightarrow 2_1^+)/B(E2;3_1^+ \rightarrow 2_2^+)$  and  $B(E2,3_1^+ \rightarrow 4_1^+)/B(E2;3_1^+ \rightarrow 2_2^+)$  for  $^{120-140}\text{Ba}$  isotopes decrease with increasing neutron number  $N$ .

The value of branching ratio  $B(E2,3_1^+ \rightarrow 2_1^+)/B(E2;3_1^+ \rightarrow 4_1^+)$  falls from the maximum value in  $^{120}\text{Ba}$  isotope at  $N = 64$  to the small values in  $^{140}\text{Ba}$  at  $N = 84$ , the experimental data exhibit the same trend of DDM values. The branching value  $B(E2,4_2^+ \rightarrow 2_1^+)/B(E2;4_2^+ \rightarrow 2_2^+)$  increased with increasing neutron number toward closed shell as well as in experimental values. The value  $B(E2,4_2^+ \rightarrow 4_1^+)/B(E2;4_2^+ \rightarrow 2_2^+)$  varying randomly as well as experimental data. The DDM values exhibit saturation in agreement with data. These values are small and fall for  $^{120-130}\text{Ba}$  isotopes, and larger for  $^{132}\text{Ba}$  isotope, and decrease again for  $^{134-140}\text{Ba}$  isotopes toward the major shell.

The ratio  $B(E2,0_2^+ \rightarrow 2_1^+)/B(E2;0_2^+ \rightarrow 2_2^+)$  is small value for all the isotopes this ratio varies slowly up to  $^{132-136}\text{Ba}$  isotopes and falls sharply thereafter, with increasing  $N$  and with increasing  $\gamma$ -softness in ( $N > 82$ )  $^{140}\text{Ba}$  isotope.

The ratio  $B(E2,2_3^+ \rightarrow 2_2^+)/B(E2;2_3^+ \rightarrow 2_1^+)$  is falling with increasing  $N$  are also reproduced in experimental values. In general the values of DDM values come closer to experimental values.

Table (6) given the quadrupole moments for ground, gamma and beta bands. In general the value of the quadrupole moment decreases monotonically for each of the states in the three bands.

Table 5: Experimental and theoretical values of Branching Ratios for Ba isotopes

Isotopes	$B(E2, 2_2^+ \rightarrow 0_1^+) / B(E2; 2_2^+ \rightarrow 0_1^+) \rightarrow$		$B(E2, 3_1^+ \rightarrow 2_1^+) / B(E2; 3_1^+ \rightarrow 2_1^+) \rightarrow$		$B(E2, 3_1^+ \rightarrow 4_1^+) / B(E2; 3_1^+ \rightarrow 4_1^+) \rightarrow$	
	Exp.	DDM	Exp.	DDM	Exp.	DDM
<sup>120</sup> Ba	-	0.311	-	0.873	-	1.21
<sup>122</sup> Ba	-	0.302	0.86	0.812	1.35	1.514
<sup>124</sup> Ba	0.17 (5)	0.221	-	0.800	-	2.41
<sup>126</sup> Ba	0.11 (2)	0.201	0.046	0.552	0.13	0.156
<sup>128</sup> Ba	0.11	0.199	0.064	0.0610	0.14	0.133
<sup>130</sup> Ba	0.054	0.096	0.038	0.0430	0.17	0.145
<sup>132</sup> Ba	0.026	0.033	0.033	0.0410	0.31	0.231
<sup>134</sup> Ba	0.006	0.0056	0.013	0.021	0.53	0.356
<sup>136</sup> Ba	-	0.0045	-	0.0034	-	0.478
<sup>140</sup> Ba	-		-	-	-	0.541

continued to Table 5

Isotopes	$B(E2, 3_1^+ \rightarrow 2_1^+) / B(E2; 3_1^+ \rightarrow 2_1^+) \rightarrow$		$B(E2, 4_2^+ \rightarrow 2_1^+) / B(E2; 4_2^+ \rightarrow 2_1^+) \rightarrow$		$B(E2, 4_2^+ \rightarrow 4_1^+) / B(E2; 4_2^+ \rightarrow 4_1^+) \rightarrow$	
	Exp.	DDM	Exp.	DDM	Exp.	DDM
<sup>120</sup> Ba	-	0.341	-	0.0065	-	0.167
<sup>122</sup> Ba	0.20	0.256	-	0.0052	-	0.336
<sup>124</sup> Ba	-	0.561	0.005	0.0061	0.29(6)	0.279
<sup>126</sup> Ba	0.40	0.472	0.008	0.0087	0.28(3)	0.267
<sup>128</sup> Ba	0.41	0.481	0.015	0.019	0.26(3)	0.261
<sup>130</sup> Ba	0.022	0.031	0.022	0.043	0.67	0.562
<sup>132</sup> Ba	0.05	0.0493	0.015	0.053	15 < 0.86	13
<sup>134</sup> Ba	0.012	0.015	0.024	0.045	0.72	0.971
<sup>136</sup> Ba	-	0.113	-	0.0066	-	1.223
<sup>140</sup> Ba	-	0.322	-	0.00742	-	2.652

Experimental are taken from refs. [31, 32, 33,]

The sign of  $Q(2_1^+, 4_1^+, 6_1^+)$  remains negative for g-band except in <sup>134-136-140</sup>Ba at neutron number  $N = 78, 80$  and  $84$ , where the very shallow oblate minimum is slightly lower than the prolate minimum. The sign of quadrupole

values for second excited states  $Q(2_2^+)$  positive in  $^{120-122-124-128-130}\text{Ba}$  isotopes and negative sign in  $^{130-140}\text{Ba}$  isotopes for the same reasons.

The sign of  $Q(2_3^+, 4_3^+, 5_1^+, 7_1^+)$  is consistently negative, but that of  $Q(4_3^+)$  varies with neutron number. This may be due to the change of nature of  $3_1^+$  and  $4_3^+$  states in certain cases.

Table 6 : Quadrupole moment for ground band, beta and gamma bands

Isotopes	$2_1^+$	$4_1^+$	$6_1^+$	$2_2^+$	$4_2^+$	$3_1^+$	$2_3^+$	$4_3^+$	$5_1^+$	$7_1^+$
$^{120}\text{Ba}$	-1.8	-1.629	-1.821	1.074	-0.521	-0.172	-1.126	-1.265	-1.20	-1.03
$^{122}\text{Ba}$	-1.49	-1.560	-1.782	0.986	-0.398	-0.162	-0.947	-1.190	-0.97	-0.95
$^{124}\text{Ba}$	-1.33	-1.388	-1.565	0.887	-0.152	0.010	-0.568	-1.150	-0.75	-0.78
$^{126}\text{Ba}$	-1.26	-1.035	-1.149	0.709	-0.0093	0.197	-0.324	0.788	-0.47	-0.51
$^{128}\text{Ba}$	-1.20	-0.65	-0.660	0.453	-0.262	0.113	-0.223	0.517	-0.28	-0.28
$^{130}\text{Ba}$	-1.11	-0.470	-0.472	0.246	-0.065	0.265	-0.226	0.408	-0.23	-0.27
$^{132}\text{Ba}$	-0.99	-0.013	-0.007	-0.015	0.043	0.273	-0.114	-0.030	-0.007	-0.007
$^{134}\text{Ba}$	-0.22	0.010	-0.008	-0.0130	0.048	0.284	-0.104	0.030	-0.008	-0.008
$^{136}\text{Ba}$	-0.20	0.0131	-0.0092	-0.0122	0.050	0.310	-0.113	0.031	-0.0083	-0.0091
$^{140}\text{Ba}$	-0.152	0.0121	-0.0099	-0.0118	0.062	0.322	-0.09	0.037	-0.0091	-0.0098

### 3-4 Magnetic Transition Probability B(M1) and Mixing Ratio

The resulting DDM calculation for B(M1) values are shown in Table (7). The results for the transitions feature for gamma band to ground band are claimed to have a collective origin. Several trends are apparent from the data in Table (7):

- (i) The magnitude of the M1 matrix elements increased with spin both gamma band to ground band transitions, in agreement with spin dependence.
- (ii) The size of gamma band to ground band matrix element seems to decrease with increasing mass number.
- (iii) The gamma-beta band M1 transitions are larger than gamma band to beta band transition by a factor of 2 to 3.

The  $\delta(E2/M1)$  multipole mixing ratios for  $^{120-140}\text{Ba}$  isotopes,  $\delta(E2/M1)$ , were calculated for some selected transitions between states. The sign of the mixing ratio must be chosen according to the sign of the reduced matrix elements. The results are listed in Table (8). The agreement with available experimental data [22,33,34,35] is more than good especially in the sign of the mixing ratio. However, there is a large disagreement in the mixing ratios of some transitions, is not due to a dominate E2 transition, but may be under the effect of very small value of M1 matrix element. However, it is a ratio between very small quantities and may change in the dominator that will have a great influence on the ratio.

For  $\gamma \rightarrow \gamma$  transitions the intraband B(E2) values have been estimated by assuming that the intrinsic E2 matrix elements in the ground and gamma bands are equal. Then combining these B(E2) values with the E2/M1 mixing ratios to the tabulated M1 transitions shown in Table (8). We note that in the DDM the intrinsic E2 matrix element of the gamma band is smaller than that of the ground band due to the finite-dimensionality of the DDM space.

Table 7: Theoretical values of Magnetic Transition Probabilities  $B(M1; J_i^+ \rightarrow J_f^+)$  in  $\mu_N^2$  Units for Ba isotopes

Isotopes	$B(M1; 2_2^+ \rightarrow 2_1^+)$	$B(M1; 3_1^+ \rightarrow 2_1^+)$	$B(M1; 3_1^+ \rightarrow 4_1^+)$	$B(M1; 4_2^+ \rightarrow 4_1^+)$
<sup>120</sup> Ba	0.0429	0.0033	0.0055	0.022
<sup>122</sup> Ba	0.0032	0.0043	0.026	1.204
<sup>124</sup> Ba	0.0157	0.00019	0.0651	0.0356
<sup>126</sup> Ba	0.0236	0.0820	0.065	0.095
<sup>128</sup> Ba	0.00040	0.0123	0.0881	0.056
<sup>130</sup> Ba	0.00040	0.0050	0.0102	0.066
<sup>132</sup> Ba	0.00065	0.009	0.0241	0.026
<sup>134</sup> Ba	0.00101	0.074	0.022	0.0101
<sup>136</sup> Ba	0.00291	0.101	0.0356	0.0241
<sup>140</sup> Ba	0.00331	0.1011	0.0432	0.076

Table 8: Experimental and theoretical values of Mixing Ratios for Ba isotopes in  $e.b/\mu_N$  Units

Isotopes	$\delta(E2, 2_3^+ \rightarrow 2_1^+)$		$\delta(E2, 2_2^+ \rightarrow 2_1^+)$		$\delta(E2, 3_1^+ \rightarrow 2_1^+)$		$\delta(E2, 3_1^+ \rightarrow 4_1^+)$		$\delta(E2, 3_1^+ \rightarrow 2_2^+)$	
	Exp.	DDM								
<sup>120</sup> Ba	-	5.23	-	10.2	-	10.3	-	1.88	-	0.121
<sup>122</sup> Ba	-	5.22	-	0.32	-	0.227	-	4.5	-	4.87
<sup>124</sup> Ba	-	1.9	-	-3.98	-	5.7	-	-3.4	-	6
<sup>126</sup> Ba	$+5_{-1}^{+2}$	4.2	-	2.89	-	14.45	-	10.2	-	12
<sup>128</sup> Ba	-	0.659	-	1.223	-	1.34	-	0.45	-	0.651
<sup>130</sup> Ba	0.296	0.541	-	3.98	$+5_{-1}^{+2}$	7	-	0.779	-	1.0
<sup>132</sup> Ba	$+8.5_{-18}^{+40}$	11	-	12.89	$+2.5_{-10}^{+10}$	3.5	-	1.451	$4.0_{-1.2}^{+1.1}$	2.12
<sup>134</sup> Ba	$-7.4_{-9}^{+9}$	-9	-	14	$+1.8_{-15}^{+1.5}$	19	-	9.77	$-17_{-6}^{+23}$	-2.16
<sup>136</sup> Ba	$-1.5_{-15}^{+6}$	2.3	-	8.3	-	-5.32	-	3.21	-	3.1
<sup>140</sup> Ba	$0.6_{-6}^{+18}$	0.998	$+0.18_{-5}^{+6}$	-	-	1.22	-	5.87	-	4.21

Experimental data are taken from refs. [22,33, 34, 35]

### CONCLUSION

We have analyzed the nuclear structure of Ba isotopes in a microscopic theory in its time dependent, two major-shell version, called the dynamic Deformation Model (DDM). This allows the nucleus to take its own shape for given  $N$  and  $Z$ . Also shape variation with spin or excitation energy is allowed although. Two input parameters have been allowed to vary within a short range are neutron number  $N$  and atomic number  $Z$ .

The Dynamic Deformation Model (DDM) calculated level energies are presented in Figs. (1) to (9). The basic features of the variation of level structure with neutron number  $N$  are well reproduced. In the ground state band the variation of the energy ratio  $E(4_1^+)/E(2_1^+)$  from a value of 2.927 in <sup>120</sup>Ba at neutron number  $N = 64$  to 2.098 in <sup>136</sup>Ba at neutron number  $N = 80$  is reproduced. The Dynamic Deformation Model (DDM) calculated level energies

are presented in Figs. (1) to (9). The basic features of the variation of level structure with neutron number  $N$  are well reproduced. In the ground state band the variation of the energy ratio  $E(4_1^+)/E(2_1^+)$  from a value of 2.927 in  $^{120}\text{Ba}$  at neutron number  $N = 64$  to 2.098 in  $^{136}\text{Ba}$  at neutron number  $N = 80$  is reproduced.

The contour plot of the potential energy surfaces  $V(\beta, \gamma)$  shows that  $^{120-140}\text{Ba}$  is a spherical nucleus and has a rotational character. with moderate deformation, was found according to the increasing neutron number.

## REFERENCES

- [1] Iachello, F and Arima A. "The Interacting Boson Mode"l. Cambridge Monographs on Mathematical Physics, (Cambridge University Press, 1987).
- [2] Iachello F. *Phys. Rev. Lett.* (2000) **85**, 2080.
- [3] Casten, R. F, Zamfir, N. V, *Phys. Rev. Lett.* (2000)**85**, 2084.
- [4] Kumar K, Gupta J. B, *Nucl. Phys.* (2000) A **694**, 199.
- [5] Kumar K, Baranger M, *Nucl. Phys.* (1968) A **110**, 529.
- [6] Puddu G, Scholten O, Otsuka T, *Nucl. Phys.* (1980)A 348 109.
- [7] Castanos O, Federman P, Frank A, Pittel S, *Nucl. Phys.* (1982) A 379 61.
- [8] Hamilton W. D, Irbäck A, and Elliott J. P, *Phys. Rev. Lett.* (1984) 53 2469.
- [9] Novoselsky A, Talmi I, *Phys. Lett.* (1986)B 172 139.
- [10] Sevrin A, Heyde K, Jolie J, *Phys. Rev.*(1987) C 36 2631.
- [11] Kumar K and Gupta J. B, *Nucl. Phys.* (2001) A 694 199.
- [12] Gupta J. B, *Phys. Rev.* (2013) C 87 64318 .
- [13] Kumar K " *Nuclear Models and the Search for Unity in Nuclear Physics* (1984) (Bergen: University of Bergen Press).
- [14] Subber A. R, Park P , Hamilton W. D, Kumar K, Schreckenback K and Colvin G **1986** *J. Phys. G : Nucl. Phys.* (1986) 12 881.
- [15] Kumar K, Remaud B, Aguer P, Vaagen J. S, Rester A. C, Foucher R and Hamilton J. H , *Phys. Rev.* (1977) C16 1253.
- [16] Kumar K, Supplement of the Progress of Theoretical Physics, (1983) Nos. 74 & 75,
- [17] Giraud B and Grammaticos B, *Nucl. Phys.* (1974) A233 373.
- [18] Lagrange Ch, Girod M, Grammaticos B and Kumar K, *Proceedings of the International Conference on Nuclear Physics, Berkeley, August 1980* (University of California, Berkeley), vol. 1, p. 352.
- [19] Kumar K, *A Study of Nuclear Deformations with Pairing Plus Quadrupole Forces* (Carnegie-Hunt Library, Pittsburgh, 1963).
- [20] Kumar K and Baranger M, *Nucl. Phys.* (1967) A92 608.
- [21] Kumar K, *The Electromagnetic Interaction in Nuclear Spectroscopy*, ed. Hamilton W D (North-Holland, Amsterdam, 1975), p. 55.
- [22] ENSDF, [http:// www.nndc.bnl.gov/ensdf](http://www.nndc.bnl.gov/ensdf) (Nuclear data sheet) (2012).
- [23] Sarkar M. S, Sen S, *Phys. Rev.* (1997) C 56 3140.
- [24] Otsuka T, Pan X. W, Arima A, *Phys. Lett.* (1990) B 247 191.
- [25] Raman S, Nestor C. W, Tikkanen P, *At. Data Nucl. Data Tables* **78**, 1 (2001).
- [26] Burnette S. M, Baxter A. M, Gyapong G. J, Fewel M. P, Spear R. H, *Nucl. Phys.* (1989) A 489 102.
- [27] Petkov P, Dewald A, Anderjtscheff W, *Phys. Rev.* (1993) C 51 2511.
- [28] Morikawa T, Oshima M, Sekine T, Hatsukawa Y, Ichikawa S, Iimura H, Osa A, Shibata M, Taniguchi A, *Phys. Rev. C* 46 (1992) R6.
- [29] Petkov P, Dewald A, Kuhn R, von Brentano P, *Phys. Rev.*(2000) C 62 014314.
- [30] Asai M, Sekine T, Osa A, Koizumi M, Kojima Y, Shibata M, Yamamoto H, Kawade K, *Phys. Rev.* (1997) C **56** 3045
- [31] Brookhaven National Laboratory, *Chart of nuclides of National Nuclear Data Center*, <http://www.nndc.bnl.gov/ENSDF/> (2010).
- [32] Bizzeti P.G *et al.*, *Phys. Rev.* (2010) C **82**, 05431.
- [33] Firestone R. B, *Table of Isotopes*, Ed. by V. S. Shirley (Wiley Intersci., New York, 1996).
- [34] Demidov A. M, Govor L. I, Kurkin V. A, and Mikhailov I. V, *Phys. At. Nucl.* (1997) **60** 503.
- [35] Lang J, Kumar K and Hamilton J. H, *Rev. Mod. Phys.* (1982) Vol.54 No.1